A Continuous Cost Function for the Reconstruction of Wired Networks from Reflection Measurements

Simon Blum, Michael Ulrich and Bin Yang

Institute for Signal Processing and System Theory, University of Stuttgart

Pfaffenwaldring 47, 70550 Stuttgart, Germany

Email: simon.blum@ikr.uni-stuttgart.de, {michael.ulrich, bin.yang}@iss.uni-stuttgart.de

Abstract—We present in this work a novel approach for the reconstruction of wired network topologies from reflection measurements. Existing approaches state the network reconstruction as discrete optimization problem, which is difficult to solve. The (discrete) topology is optimized while the cable lengths are a secondary result.

The contribution of this paper is the formulation of the topology reconstruction as a continuous problem. The idea is to rather optimize the (continuous) cable lengths and automatically obtain the topology as a secondary result. Further we present a heuristic algorithm to solve the optimization approximately. Using simulated reflectometry data, we demonstrate the performance of our approach.

I. Introduction

The reconstruction of the topology and cable lengths of wired networks is of interest for many purposes. Applications reach from fault detection in power grids [1] over communication network diagnosis for airplanes or automobiles [2], [3] to the identification of unknown communication networks [4], [5].

One possibility for fault location is the comparison of measured reflections to a reference reflection measurement of a healthy network followed by a localization technique where the topology of the healthy network is a priori known [2], [3]. Unfortunately, measurements of the healthy network are not always available.

Another possibility is to equip all cable ends with devices for distance measurement. The rooted neighbor-joining algorithm (RNJA) [6], [5], [4] is able to determine the network topology uniquely and with low computational effort, however communicating measurement devices at all leaf nodes of the network are often not realizable. Cables without measurement devices can not be detected by RNJA or its improved version [7].

Finally, the topology reconstruction from a single [1], [8] or multiple [9] reflection measurements does not require any prior knowledge about the network or difficult distance measurements of cable ends. Reflectometry is a powerful tool to obtain information about the structure of a cable network. Though commercial applications evaluate only the first reflection to determine the distance to the nearest discontinuity on the cable, recent approaches aim to reconstruct the whole network structure. However, the problem of [1], [9], [8] is that the estimation of the topology is a discrete problem (a cable can either exist or not). An exhaustive search to try out all combinations of cables (topologies) is computationally complex. Hence [1], [9], [8] present iterative heuristics to approximate the combinatory problem. Though [8] reduces

the number of possible topologies in comparison to [1] by an additional plausibilisation of each iteration, [9] rather keeps the most likely candidate of each iteration, resulting in an unique solution. Another problem of [1], [8] is that they strongly rely on a perfect resolution of all reflections (all reflections can be distinguished). In practice, this is usually not achievable due to limited bandwidth and dispersion of the cables.

In this paper, we formulate the discrete estimation problem of [1], [9], [8] as a continuous problem, by optimizing the cable lengths of a generic topology rather than the topology itself. The idea is that a sufficiently large binary tree can represent any topology by allowing cables with length of zero. The optimization goal is to minimize the difference of a single reflection measurement and simulated reflections from the candidate. To solve this non-convex optimization problem, we present an iterative approach. In contrast to [1], [9], [8] our algorithm does not rely on the detection of single reflections, hence it is easier to cope with overlapping reflections caused by limited resolution or dispersion.

We use the following notations: Underlined variables denote vectors or sets. $(\cdot)^{\mathsf{T}}$ stands for transpose while $\|\cdot\|$ is the Euclidean norm. The imaginary unit is denoted by j.

The rest of this paper is organized as follows: Sec. II revises the signal model for the reflectometry. The network reconstruction problem is formulated in Sec. III. An iterative algorithm to solve it is presented in Sec. IV. We show simulation results in Sec. V and Sec. VI concludes the paper.

II. Signal Model

We assume that the network structure can be modeled as a tree topology, where inner nodes represent junctions, leaf nodes cable ends and edges cables. Further we assume that each cable has approximately the same characteristic impedance Z_0. We neglect junctions of only two cables, as they are immeasurable discontinuities for reflectometry. Also we assume that only the leaf nodes of the network are connected to load, which has, compared to the characteristic impedance of the wire, either a very high or a very low impedance. We approximate the cable ends by an open end (reflection coefficient $\Gamma = 1$) or short circuit ($\Gamma = -1$) respectively [10]. These assumptions hold for many communication or secondary power distribution networks.

Among others, well known reflectometry methods are time domain reflectometry (TDR) and frequency domain reflectometry (FDR) (see [11] for an overview). The algorithm proposed in this work can be easily modified for any reflectometry method. In this work we choose FDR, because
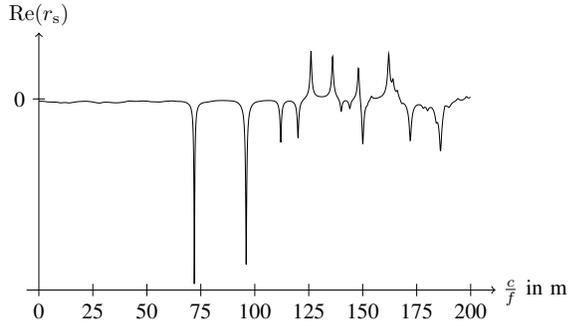
Fig. 1. Example for a simulated FDR measurement with limited bandwidth and dispersive cables. It can be observed that distant reflections overlap due to dispersion and can not be resolved. c is the propagation speed of the electromagnetic wave on the cable.
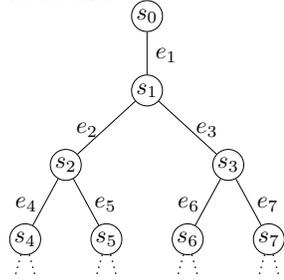

Fig. 2. Generic network structure

- with FDR a more realistic model is possible because dispersion and attenuation can be modeled by a frequency dependent (complex) propagation parameter $\gamma(f)$ and
- with FDR a more accurate model is possible because in frequency domain a finite term is sufficient to model the reflections, while in time domain an infinite series would be necessary.

Fig. 1 shows the result of a simulated FDR measurement. Existing commercial methods simply evaluate the first reflection to detect errors on the cable directly connected to the measurement device. In contrast, the objective of this paper and other recent approaches is to reconstruct the complete network.

A FDR measurement is performed by evaluating a frequency sweep at K frequencies,

$$\underline{f} = [0, f_{\mathrm{s}}, 2f_{\mathrm{s}}, ..., (k-1)f_{\mathrm{s}}, ..., (K-1)f_{\mathrm{s}}]^{\mathsf{T}}, \qquad (1)$$

at the measurement node of the network. The frequency sweep is sent at the measurement node and the received signal corresponds to the channel response at the measurement node. The complex reflection coefficient $\Gamma_{\mathrm{m}}(k)$ for the k-th frequency $f_{\mathrm{k}} = (k-1)f_{\mathrm{s}}$ is measured by calculating the correlation between the sent and received signal or in hardware by mixing the sent and received signal, low-pass filtering and sampling. All $\Gamma_{\mathrm{m}}(k)$ can be concatenated to one measurement vector $\underline{\Gamma}_{\mathrm{m}} = [\Gamma_{\mathrm{m}}(1), ..., \Gamma_{\mathrm{m}}(k), ..., \Gamma_{\mathrm{m}}(K)]^{\mathsf{T}}$. The measured signal in time domain $\underline{r}_{\mathrm{m}}$ is calculated by applying an inverse discrete Fourier transform (IDFT) to $\underline{\Gamma}_{\mathrm{m}}$.

$$\underline{r}_{\mathrm{m}} = \mathrm{IDFT}(\underline{\Gamma}_{\mathrm{m}}) \qquad (2)$$

A method for the simulation of FDR measurement was proposed in [10]. It is based on the calculation of the frequency-dependent reflection coefficient $\Gamma_{\mathrm{s}}(k)$ at the measurement point for the entire network. The idea is that the reflection coefficient of a node can be expressed in terms of the reflection coefficients of neighboring nodes and cable lengths.

In an iterative procedure, the reflection coefficients of the nodes are transformed over a wire according to

$$\Gamma_{\mathrm{b}}(u,k) = \Gamma_{\mathrm{e}}(u,k) \cdot \mathrm{e}^{-2\vartheta_{\mathrm{u}}\gamma(f_{\mathrm{k}})}, \qquad (3)$$

where $\Gamma_{\mathrm{e}}(u,k)$ is the reflection coefficient at the end of the wire with index u for the k-th frequency, $\Gamma_{\mathrm{b}}(u,k)$ is the reflection coefficient at its origin and ϑ_u denotes the wire length. The reflection coefficient $\Gamma_{\mathrm{b}}(u,k)$ can be converted to an impedance $Z_{\mathrm{b}}(u,k)$ using eq. 4a and the impedances $Z_{\mathrm{b}}(1,k)$ and $Z_{\mathrm{b}}(2,k)$ of two neighboring wires can be combined by setting the impedances into parallel (eq. 4b). Then the resulting impedance $Z_{\mathrm{e}}(v,k)$ can be converted back to a reflection coefficient $\Gamma_{\mathrm{e}}(v,k)$, eq. 4c.

$$Z_{\mathrm{b}}(u,k) = Z_0 \frac{1 + \Gamma_{\mathrm{b}}(u,k)}{1 - \Gamma_{\mathrm{b}}(u,k)} \qquad (4a)$$

$$Z_{\mathrm{e}}(v,k) = \frac{Z_{\mathrm{b}}(1,k)Z_{\mathrm{b}}(2,k)}{Z_{\mathrm{b}}(1,k) + Z_{\mathrm{b}}(2,k)} \qquad (4b)$$

$$\Gamma_{\mathrm{e}}(v,k) = \frac{Z_{\mathrm{e}}(v,k) - Z_0}{Z_{\mathrm{e}}(v,k) + Z_0} \qquad (4c)$$

Combining eq. 4a, eq. 4b and eq. 4c yields

$$\Gamma_{\mathrm{e}}(v,k) = \frac{\Gamma_{\mathrm{b}}(1,k) + \Gamma_{\mathrm{b}}(2,k) + 3\Gamma_{\mathrm{b}}(1,k)\Gamma_{\mathrm{b}}(2,k) - 1}{\Gamma_{\mathrm{b}}(1,k) + \Gamma_{\mathrm{b}}(2,k) - \Gamma_{\mathrm{b}}(1,k)\Gamma_{\mathrm{b}}(2,k) + 3} . (5)$$

As an example, in Fig. 2 the reflection coefficients of nodes s_4 and s_5 are transformed to node s_2 using eq. 3. Then the reflection coefficient of node s_2 can be calculated with eq. 5, which already includes the effect of edges e_4 and e_5. By iteratively combining and transforming reflection coefficients towards the measurement node, the reflection coefficient at the measurement node $\Gamma_{\mathrm{s}}(k)$ of the whole network can be calculated. This procedure is repeated for all frequencies of $\underline{f}$ and the resulting $\Gamma_{\mathrm{s}}(k)$ are stacked in one vector $\underline{\Gamma}_{\mathrm{s}} = [\Gamma_{\mathrm{s}}(1), ..., \Gamma_{\mathrm{s}}(k), ..., \Gamma_{\mathrm{s}}(K)]^{\mathsf{T}}$. An IDFT yields the time domain reflection signal of the simulated measurement

$$\underline{r}_{\mathrm{s}} = \mathrm{IDFT}(\underline{\Gamma}_{\mathrm{s}}). \qquad (6)$$

For a more detailed description of FDR, we refer the interested reader to [1], [10]. With this underlying physical model, we assume that

$$\underline{\Gamma}_{\mathrm{m}} = \underline{\Gamma}_{\mathrm{s}} + \underline{N}, \qquad (7)$$

where $\underline{N}$ is i.i.d. white Gaussian noise, e.g. from amplifiers and other electronic circuits in the FDR measurement device. According to eq. 2,

$$\underline{r}_{\mathrm{m}} = \underline{r}_{\mathrm{s}} + \underline{n}, \qquad (8)$$

where $\underline{n}$ is the spectrum of $\underline{N}$.

III. NETWORK RECONSTRUCTION PROBLEM

Existing approaches for the reconstruction of a networks topology from reflection measurement are based on a discrete optimization problem. The algorithms primarily try to reconstruct the topology, where a cable can either exist or not exist. The cable length is just a secondary result. The examination of all combinatorial possibilities to solve the problem perfectly is computationally costly, hence only heuristic approaches exist.
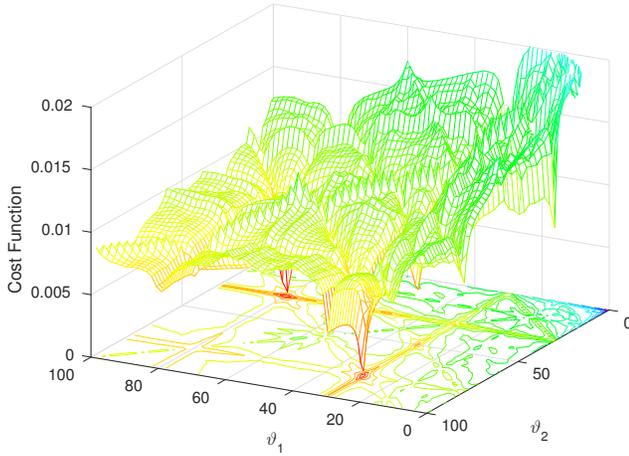
Fig. 3. Cost function of eq. 9 for two cable lengths $\vartheta_1 = 30$ and $\vartheta_2 = 80$, if all other parameters were perfectly known.

---

input: Reflection measurement $\underline{r}_\mathrm{m}$
output: Optimization result $\hat{\underline{\vartheta}}$, $\hat{\underline{z}}$
1: initialize set of candidate edges $\underline{e} = \{e_1\}$
2: **while** $\underline{e} \neq \emptyset$ **do**
3: find edge e_l in $\underline{e}$ with nearest parent node
4: determine $\hat{\vartheta}_l, \hat{z}_l = \arg\min_{\vartheta_1, z_1} \|\underline{r}_\mathrm{m} - \underline{r}_\mathrm{s}(\vartheta, \underline{z})\|^2$
5: choose the edge e_n minimizing eq. 9 for $\hat{\vartheta}_l$ and $\hat{z}_l$
6: try to find inner node on new edge
7: **if** values for e_n improve the cost function **then**
8:   add values for e_n to $\hat{\underline{\vartheta}}$ and $\hat{\underline{z}}$
9:   add new candidates to $\underline{e}$
10: **end if**
11: $\underline{e} = \underline{e} \setminus \{e_\mathrm{n}\}$
12: **end while**

Fig. 4. Topology reconstruction algorithm

IV. NETWORK RECONSTRUCTION ALGORITHM

Our iterative approach is sketched in Fig. 4. In each iteration one edge of the topology is examined to avoid the computational complexity of the maximum likelihood estimator (eq. 9) directly. With the sequential examination of the edges we separate the degrees of freedom of eq. 9. We solve L cost functions depending on one edge rather than solving one cost function depending on all edges. The separation of the optimization variables is motivated by the structure of the cost function. The example in Fig. 3 shows that the cost functions has clear trenches parallel to the axes, hence the coupling of the parameters is rather loose.

The set $\underline{e}$ contains the candidate edges that still have to be examined in the following iterations. Initially the set $\underline{e}$ contains only the edge which is directly connected to the measurement node of the network.

One iteration consists of six steps. In the first step (line 3) the candidate edge e_l of $\underline{e}$ whose parent node is nearest to the measurement node is selected. This will give the most general result in the following optimization step.

The second step is the estimation of the wire length ϑ_l and node impedance z_l for the selected candidate edge in line 4. In contrast to eq. 9, the cost function is optimized only for a single element ϑ_l of $\underline{\vartheta}$ resulting in a considerable reduction of the computational effort. For the values of z_l we consider three possibilities, namely $z_l = 0$ and $z_l = \infty$ for cable ends (see Sec. II) or $z_l = \frac{1}{2} Z_0$ if s_l represents a junction. The parameter ϑ_l is considered as continuous. The estimation of ϑ_l is implemented with three independent optimizations for all choices of $z_l \in \{0, \frac{1}{2} Z_0, \infty\}$. A grid search is performed to find an initial estimate followed by a local (gradient-based) optimization for refinement. As the optimization appends an additional wire to the network, the impedance of the parent node of the candidate edge has to be corrected. If the degree of the parent node is 3, its impedance has to be set to ∞, if the parent nodes degree is 2, its impedance has to be set to Z_0.

The third step (line 5) checks if there is another candidate edge e_n in $\underline{e}$ which gives a better cost value than e_l. For this purpose we create a candidate for all N edges in $\underline{e}$. The length of related edge $\hat{\vartheta}_\mathrm{n}$ is chosen such that the distance

---

In contrast to the existing approaches we formulate a continuous optimization problem for the reconstruction of the topology of a wired network. For this purpose, we choose a binary tree as the topology of the network model, as depicted in Fig. 2. The model parameters are the (continuous) cable length ϑ_l of edge e_l and the node impedance z_l of node s_l. As the networks leaf node impedances are usually much higher or much lower than Z_0, we approximate them by $z_l \in \{0, \infty\}$. The lengths of all edges can be stacked in one parameter vector $\underline{\vartheta} = [\vartheta_l]^\mathsf{T}$ and the node impedances in $\underline{z} = [z_l]^\mathsf{T}$. The topology itself is not a model parameter with this approach.

Though the true topology may be different from a binary tree, we can still apply the presented model by setting certain cable lengths to zero. If, for example in Fig. 2, a junction of 4 wires shall be resembled at the node s_1, the wire length ϑ_2 of edge e_2 of the network can be set to zero. The resulting network generates the same reflectometry signal as if the edges e_3, e_4 and e_5 were connected directly to the end of the first wire e_1 from the measurement node.

With this novel model the maximum likelihood estimator of $\underline{\vartheta}$ is

$$\hat{\underline{\vartheta}} = \arg\min_{\underline{\vartheta}, \underline{z}} \|\underline{r}_\mathrm{m} - \underline{r}_\mathrm{s}(\underline{\vartheta}, \underline{z})\|^2 \qquad (9)$$

where $\underline{r}_\mathrm{s}(\underline{\vartheta}, \underline{z})$ is the FDR simulation model of Sec. II with the parameters $\underline{\vartheta}$ and $\underline{z}$.

An examination of eq. 9 shows that the optimization problem is non-convex in $\underline{\vartheta}$ due to the nonlinear function $\underline{r}_\mathrm{s}(\underline{\vartheta}, \underline{z})$. An example of the cost function is depicted in Fig. 3.

Unfortunately finding $\hat{\underline{\vartheta}}$ in eq. 9 using an exhaustive search is only feasible for very small topologies. To find $\hat{\underline{\vartheta}}$ in eq. 9, a grid search with M points for each element ϑ_l of $\underline{\vartheta}$ would be necessary. When L is the number of cables considered in the binary tree this would lead to a total number of M^L grid search points resulting in a computational complexity of $\mathcal{O}(M^L)$ for the exhaustive search. A heuristic approach to approximate eq. 9 by iteratively optimizing the elements of $\underline{\vartheta}$ and $\underline{z}$ with a complexity of $\mathcal{O}(LM + L^2)$ is presented in the following section.

from the measurement node and the leaf node of e_n and e_l are equal. The candidate topology yielding the lowest cost function value (eq. 9) is chosen in this step. The result is refined by an additional local optimization of eq. 9 over $\underline{\vartheta}$ using the calculated edge lengths $\hat{\vartheta}_n$ as initial value.

One problem of the iterative estimation (separate optimization of the edges) arises from the fact that a cable end with $z = \{0, \infty\}$ can cause a reflection of higher amplitude than that of an inner node (junction) which is closer to the measurement node. The iterative procedure then might prefer a solution which omits the inner node and resembles the reflection caused by the cable end as this will lead to the higher improvement of the cost function.

We account for this problem in the fourth step (line 6) by searching for an inner node which splits the new edge into two parts. Therefore another edge e_{2n} is appended at the node s_n with a new end node s_{2n}. The search is implemented by an optimization of parameter $t \in [0, 1]$ with $z_n = Z_0$, $z_{2n} = \hat{z}_n$, $\vartheta_n = t\hat{\vartheta}_n$ and $\vartheta_{2n} = (1-t)\hat{\vartheta}_n$. The optimization is (like in the second step) implemented by a grid search over t followed by a local (gradient-based) optimization resulting in value $\hat{t}$. If such a node is found, i.e. the cost function of the split edge is better than that for the single edge, ϑ_n is set to $\hat{t}\hat{\vartheta}_n$ and z_n is set to $\frac{1}{2}Z_0$.

In the fifth step (lines 7 to 10) the convergence of the algorithm is evaluated. If the cost function value with the additional edge found in this iteration is better than that of the previous iteration, the new edge is added to the topology. Candidate edges for the following iterations are added to $\underline{e}$, if the end of the new edge is an inner node ($\hat{z}_n = \frac{1}{2}Z_0$).

In the last step (line 11) the edge e_n is removed from the set of candidate edges. The algorithm terminates if the set of candidate edges is empty.

V. EXPERIMENTS

In our experiments we performed simulations using a MATLAB implementation of the proposed algorithm. A set of 1000 random networks with a given number of nodes is generated as test cases for the simulations. The wire lengths of the networks are uniformly distributed between 10 and 100 m. In our simulations, we use the (dispersive) propagation parameter $\gamma(f_k) = 6.271 \cdot 10^{-08} f_k^{0.6702} + \mathrm{j}\, 2.768 \cdot 10^{-08} f_k$, which we measured for a cable of type RG58U. The algorithm uses a simulated measurement to perform the reconstruction of the networks topology and wire lengths.

As for a reflection measurement the power of the measured signal $\underline{r}_m$ depends on the structure of the network, we rather use the power of the sent signal as reference for the SNR. We define the SNR $= \frac{A_s^2}{\sigma^2}$ with respect to the sent signal amplitude A_s and noise variance σ^2.

To evaluate the quality, the reconstructed network is compared to the original. As in [9], we use the two scores α_c and α_s for that purpose. The percentage of networks that are completely reconstructed is given by the score α_c. The second score α_s denotes the similarity between the original and the reconstructed network. A metric based on the size of the maximum common subtree (mcs) from [12] is used to calculate α_s. When G_1 is the graph of the original network and G_2 is the graph of the reconstructed network and the order

$|G|$ of a graph denotes the number of its edges, the score α_s is calculated as follows:

$$\alpha_s = \frac{|\mathrm{mcs}(G_1, G_2)|}{\max(|G_1|, |G_2|)} \tag{10}$$

In order to compare the results of the proposed algorithm to that of an existing approach we also examined the algorithm which is presented in [1]. The ideal reflectometry model used in [1] yields all reflections at the measurement node (with limited number of reflections per branch) with exact locations. It is assured that all reflections can be resolved, no matter how close to each other they are and how low the signal amplitude is. In practice, reflections are damped by the cable attenuation and can not be resolved if they are close to each other due to limited measurement bandwidth and dispersion. These effects are however contained in the simulation model in Sec. II. To apply [1] with our simulation model, we use a simple peak detection algorithm, where peaks need to be at least 1 m away from each other and the amplitude must be higher than $5 \cdot 10^{-5}$ times the amplitude of the sent signal.

The algorithm which is presented in [1] contains a consistency check for systematically created candidate topologies which is not further explained. If all reflections were resolved perfectly, the consistency check could simply be done by comparing simulated reflections of a candidate topology to the measured reflections. If all simulated reflections are contained in the measured reflections, the candidate topology can be considered as consistent. However, if not all reflections can be resolved due to the more realistic FDR simulation of Sec. II, the algorithm of [1] would mostly fail to reconstruct any network, as valid candidate topologies are likely to be rejected by the consistency check.

To be able to compare our method to [1], we introduce a consistency quota q (ratio of the number of consistent reflections and the number of simulated reflections). A measured and a simulated reflection are considered consistent, if their distance is less than 1 m. Only if the consistency quota of a candidate topology is lower than a certain value, the topology is rejected by the consistency check. Similarly to [1], we terminate the algorithm if there are more than 300 candidate topologies and return all candidates as the result.

As all consistent candidate topologies are considered as valid, the result of the algorithm from [1] might be ambiguous. For that reason we use the scores $\bar{\alpha}_c$, $\tilde{\alpha}_c$, $\bar{\alpha}_s$, and $\tilde{\alpha}_s$ to evaluate the results. While $\bar{\alpha}_c$ denotes the percentage of completely reconstructed networks taking the average of all α_c if a reconstruction was ambiguous, $\tilde{\alpha}_c$ considers the best α_c of all ambiguous reconstructions. To achieve $\tilde{\alpha}_c$ in practice, an algorithm to perfectly choose the topology would be still necessary. $\bar{\alpha}_s$ denotes the similarity between the original and the reconstructed network taking the mean of all result topologies of a test case, $\tilde{\alpha}_s$ only considers that result topology of a test case which has the highest α_s.

In our first experiment we performed simulations with a bandwidth of 500 MHz in the simulated FDR measurement. The simulations were performed on networks consisting of 6 nodes with $K = 8192$ equidistant measurement points in the simulated FDR measurement. For the algorithm of [1] we tried all combinations of $q \in \{10\,\%, 15\,\%, ..., 95\,\%\}$ and the maximum reflection distance $r_{\max} \in \{400\,\text{m}, 500\,\text{m}, ..., 1000\,\text{m}\}$.

TABLE I
COMPARISON OF THE PROPOSED ALGORITHM AND THE METHOD OF [1]

proposed algorithm		algorithm from [1]			
α_s [%]	α_c [%]	$\tilde{\alpha}_s$ [%]	$\tilde{\alpha}_c$ [%]	$\bar{\alpha}_s$ [%]	$\bar{\alpha}_c$ [%]
84.5	71.3	74.8	34.7	36.4	0.06

TABLE II
SIMULATION RESULTS FOR DIFFERENT NOISE LEVELS AND BANDWIDTHS
IN THE SIMULATED MEASUREMENT

BW	1 GHz		500 MHz		250 MHz	
SNR	α_s [%]	α_c [%]	α_s [%]	α_c [%]	α_s [%]	α_c [%]
24 dB	67.9	44.1	77.8	58.0	73.4	55.3
30 dB	84.1	68.8	83.0	68.2	75.0	59.5
∞	85.7	72.7	84.5	71.3	75.4	60.7

TABLE III
SIMULATION RESULTS FOR DIFFERENT NETWORK SIZES

Network size	6 nodes		8 nodes	
	α_s [%]	α_c [%]	α_s [%]	α_c [%]
	84.5	71.3	68.4	39.5

The highest sum of $\tilde{\alpha}_s$ and $\tilde{\alpha}_c$ was achieved for $q = 20\%$ and $r_{\max} = 900\,\mathrm{m}$, for which we show the results in Table I, alongside with the results of the proposed algorithm.

The introduction of the consistency quota into the algorithm of [1] on the one hand allows us to apply it to a more realistic reflectometry model, but on the other hand weakens the consistency check. This leads to a higher ambiguity of the reconstruction results. The high ambiguity can be seen by the ratio between the scores with perfect selection of the best result topology ($\tilde{\alpha}_s$ and $\tilde{\alpha}_c$) and the scores that consider all result topologies ($\bar{\alpha}_s$ and $\bar{\alpha}_c$). Compared to the scores $\tilde{\alpha}_s$ and $\tilde{\alpha}_c$ the proposed algorithm shows significantly better results in both scores α_s and α_c. Even if a perfect choice of the ambiguously reconstructed topologies would be possible the reconstruction rate of proposed approach is almost 10% higher than for [1].

This can be explained by the formulation of the cost function in eq. 9. The proposed method does not require a peak detection step and is hence more robust to overlapping reflections. Further the continuous nature of eq. 9 is beneficial for the algorithm in Fig. 4.

In our second experiment we performed simulations with different bandwidths and noise levels to evaluate the influence of these factors. The bandwidth BW ranges from 250 MHz to 1 GHz. We simulate networks for a SNR of 24 dB and 30 dB. For comparison, we also performed simulations for each bandwidth without noise. The simulations were performed on networks consisting of 6 nodes with $K = 8192$ equidistant measurement points in the simulated FDR measurement.

The results of the second experiment are shown in Table II. As it is to be expected the scores for a given bandwidth are decreasing for increasing noise. It can be observed that increasing the bandwidth beyond 500 MHz does not result in a significant improvement of the reconstruction rate. Though the resolution of the FDR measurement increases with the

bandwidth, the attenuation of the cable is strong for high frequencies, such that almost no additional information can be obtained.

In our third experiment we performed simulations with different network sizes to evaluate the effect on the reconstruction. Each simulation was performed with a measurement bandwidth of 500 MHz, 8192 measurement points and without noise. We performed simulations with network sizes of 6 and 8 nodes. The results are shown in Table III. The network size has a strong effect on the percentage of completely reconstructed networks. The reason is that for a network with more nodes, the reflections are more likely to be unresolvable, especially for cables far from the measurement node (cf. far reflections in Fig. 1). However, α_s indicates that most cables near to the measurement node were reconstructed, even for a large network.

VI. SUMMARY

A novel approach for the inference of a passive wired networks topology is proposed in this work. In contrast to existing solutions, dispersive cables and limited resolution were considered. Moreover, the network reconstruction is stated as a continuous problem. An iterative heuristic to solve the reconstruction problem is presented. Experiments based on simulated reflection measurements show that the proposed algorithm outperforms existing solutions by almost 10%.

REFERENCES

[1] M. Ahmed and L. Lampe, "Power line network topology inference using Frequency Domain Reflectometry," *IEEE International Conference on Communications (ICC)*, pp. 3419–3423, June 2012.

[2] M. K. Smail, L. Pichon, M. Olivas, F. Auzanneau, and M. Lambert, "Reconstruction of faulty wiring networks using reflectometry response and genetic algorithms," *International Journal of Applied Electromagnetics and Mechanics*, vol. 35, no. 1, pp. 39–55, 2011.

[3] W. B. Hassen, F. Auzanneau, L. Incarbone, F. Pérès, and A. P. Tchangani, "Distributed sensor fusion for wire fault location using sensor clustering strategy," *International Journal of Distributed Sensor Networks*, vol. 2015, p. 54, 2015.

[4] M. Ahmed and L. Lampe, "Power line communications for low-voltage power grid tomography," *IEEE Transactions on Communications*, vol. 61, no. 12, pp. 5163–5175, December 2013.

[5] L. Lampe and M. Ahmed, "Power grid topology inference using power line communications," *IEEE International Conference on Smart Grid Communications (SmartGridComm)*, pp. 336–341, Oct 2013.

[6] J. Ni and S. Tatikonda, "Network tomography based on additive metrics," *IEEE Transactions on Information Theory*, vol. 57, no. 12, pp. 7798–7809, 2011.

[7] X. Ma, F. Yang, W. Ding, and J. Song, "Topology reconstruction for power line network based on Bayesian compressed sensing," *International Symposium on Power Line Communications and its Applications (ISPLC)*, pp. 119–124, March 2015.

[8] C. Zhang, X. Zhu, Y. Huang, and G. Liu, "High-resolution and low-complexity topology estimation for power line communication networks," *IEEE International Conference on Communications (ICC)*, pp. 4925–4930, June 2015.

[9] M. Ulrich and B. Yang, "Inference of wired network topology using multipoint reflectometry," *23rd European Signal Processing Conference (EUSIPCO)*, pp. 1965–1969, May 2015.

[10] F. Auzanneau, M. Olivas, and N. Ravot, "A simple and accurate model for wire diagnosis using reflectometry," *PIERS Proceedings*, pp. 232–236, 2007.

[11] M. Smail, L. Pichon, M. Olivas, F. Auzanneau, and M. Lambert, "Recent progress in wiring networks diagnosis for automotive applications," *COMPEL - The international journal for computation and mathematics in electrical and electronic engineering*, vol. 30, no. 4, pp. 1148–1161, 2011.

[12] H. Bunke and K. Shearer, "A graph distance metric based on the maximal common subgraph," *Pattern Recognition Letters*, vol. 19, no. 34, pp. 255–259, 1998.